Journal of Nuclear Materials 445 (2014) 218–223

Contents lists available at ScienceDirect

Journal of Nuclear Materials

journal homepage: www.elsevier.com/locate/jnucmat

Investigation of powdering ductile gamma U-10 wt%Mo alloy for dispersion fuels

R.M. Leal Neto [a,*], C.J. Rocha [a], E. Urano de Carvalho [a,b], H.G. Riella [b,c], M. Durazzo [a,b]

[a] Nuclear and Energy Research Institute, IPEN/CNEN-SP, São Paulo, Brazil
[b] Science and Technology Brazilian Institute, Innovating Nuclear Reactors, Brazil
[c] Chemical Engineering Department, Santa Catarina Federal University, Florianópolis, Brazil

ARTICLE INFO

Article history:
Received 21 December 2012
Accepted 11 November 2013
Available online 20 November 2013

ABSTRACT

This work forms part of the studies presently ongoing at Nuclear and Energy Research Institute – IPEN/CNEN-SP investigating the feasibility of powdering ductile U-10 wt%Mo alloy by hydriding–milling–dehydriding of the gamma phase (HMD). Hydriding was conducted at room temperature in a Sievert apparatus following heat treatment activation. Hydrided pieces were fragile enough to be hand milled to the desired particle size range. Hydrogen was removed by heating the samples under high vacuum. X-ray diffraction analysis of the hydrided material showed an amorphous-like pattern that is completely reversed following dehydriding. The hydrogen content of the hydrided samples corresponds to a trihydride, i.e. $(U,Mo)H_3$. SEM analysis of HMD powder particles revealed equiaxial powder particles together with some plate-like particles. A hypothesis for the amorphous hydride phase formation is suggested.

1. Introduction

For the last 30 years, high uranium density dispersion fuels have been developed in order to achieve the low enrichment goals of the Reduced Enrichment for Research and Test Reactors (RERTR) Program. Gamma U–Mo alloys, particularly those with 7–10 wt%Mo, as a fuel phase dispersed within an aluminum matrix have shown good results regarding their performance in irradiation tests [1,2]. These results have encouraged us to consider the use of this alloy in the nuclear fuel for the Brazilian Multipurpose Research Reactor (RMB), currently being designed. Gamma U–Mo alloys are planned for the second stage of the reactor operation, since uranium silicide, U_3Si_2, already produced in Brazil, will be used initially.

Powdering U–Mo alloys is a major concern when fuel fabrication is based on the dispersion technology. There are at least three main process routes by which ductile (and tough) gamma U–Mo alloys can be powdered: atomization (mainly centrifugal atomization) by the rotating disk method [3] or the rotating electrode process [4]; mechanical comminution, i.e. machining or grinding [5,6]; and chemical comminution, i.e. the hydriding–dehydriding process, also known by its acronym HDH or HD [7–12], or as HMD when a milling operation is performed between these treatments. Atomization was discarded since it is too expensive.

Previous reports on mechanical grinding [5,6] show conflicting results. In the paper by Vacelet et al. [6], the specific grinding method was not mentioned. Ground U–Mo powder particle morphology was shown in a low resolution photograph with no magnification scale. The particles appear to be platelets and seem to be too large, a fact that can be inferred from the micrographs of the longitudinal sections of the fuel plates showing the meat thickness, despite the continued absence of the magnification scales. Clark et al. [5] used a rotary file powdered by a small hobby lathe to grind the alloy slug into powder form. The particles produced by this method are shavings (size range in mm) which were sieved to obtain the powder size fraction required for fuel plate production. Although a greater rotation speed was able to reduce the powder particle size, the authors argued that this was insufficient to recommend this route for production scale powder fabrication, because the production rate is slow. Other disadvantages are also presented, such as a high degree of contamination (undefined) from the grinding bit and the production of particles with high dislocation density, which may lead to nucleation sites for fission gas bubble formation during irradiation [5]. On the other hand, this high concentration of defects was later presented as a possible advantage by trapping gas atoms and developing an oxide layer on the surface of the ground UMo particles that apparently has a positive effect on the mechanical properties of the interaction layer with the aluminum matrix under hot irradiation conditions [13].

* Corresponding author. Address: Av. Prof. Lineu Prestes, 2242, Cidade Universitária, CEP 05508-000, São Paulo, SP, Brazil. Tel.: +55 11 31339218; fax: +55 11 31339280.
E-mail address: lealneto@ipen.br (R.M. Leal Neto).

0022-3115/$ - see front matter © 2013 Elsevier B.V. All rights reserved.
http://dx.doi.org/10.1016/j.jnucmat.2013.11.014

Following the hydriding route, the U–Mo alloy pieces are embrittled by hydrogen (hydriding stage) and can then be ground mechanically with the aid of a low impact mill (rod or knife mill) or manually with the aid of a hand mortar, producing powder particles that are first sieved and finally dehydrided (dehydriding stage). This route has at least two approaches that can be indicated, depending on what phases are present during the adsorption of hydrogen: hydriding gamma U–Mo alloy containing some alpha phase at grain boundaries and hydriding gamma phase alone (massive hydriding).

The first approach, named HD, is based on an easier process, in which strong hydrogen intake by the alpha Uranium phase (orthorrombic) occurs, forming UH_3 and an embrittled material [7,8]. Initially a heat treatment (annealing) is conducted to grow the gamma grains to the desired particle size range. A second heat treatment is necessary to precipitate the alpha Uranium phase at prior gamma grain boundaries. By treating this material with hydrogen, UH_3 is formed at the grain boundaries, pulverizing the alloy by intergranular fracture, making a milling operation unnecessary. The resulting particles should be small monocrystals within the size range developed at the annealing heat treatment [7].

The second approach was named HMD and combines hydriding–dehydriding with a milling process. Gamma U–Mo alloys are directly hydrided, with no gamma to alpha phase transformation, but powder can only be produced by interposing a milling operation before dehydriding. To achieve the gamma phase hydriding, a prior heat treatment is necessary to activate the material. Pasqualini et al. [10] reported for the first time that after heating the material to 700 °C (1 h), it was able to absorb hydrogen during cooling at a temperature range between 190 and 50 °C. The hydriding of gamma U–Mo is controlled by hydrogen diffusion but, because of the high density difference between the alloy and the hydride, internal cracks and fractures are formed parallel to the diffusion front and new surface is formed. The consequence is that the rate of hydride formation is greater than the expected by the diffusion process. The authors argued that beta U–Mo hydride (A-15 structure) is formed causing embrittlement of the alloy [10].

More recently, Chen et al. (2010) verified that after a heating to 600 °C under vacuum, alloy samples showed increased absorption of hydrogen at room temperature during successive hydriding–dehydriding cycles, until saturation was achieved after 8 cycles of hydriding at room temperature and 0.5 MPa dehydriding at 600 °C under vacuum [11]. Moreover, Yi-Fu et al. (2010) demonstrated that activation could be obtained by careful chemical cleaning of the alloy surface followed by heating to only 250 °C under vacuum, after which samples could be hydrided at room temperature [12].

In a previous study, our group obtained U10Mo powder by hydrogenation–milling–dehydrogenation (HMD). We adopted the term "hydrogenation", since there was no evidence of the formation of a hydride phase. High-energy ball-milling was used in order to achieve comminution of the hydrogenated material [14]. In this investigation, we obtained a powdered U-10 wt%Mo alloy by hydriding the gamma phase after a thermal activation process. Once activated, the samples were able to absorb hydrogen at room temperature. The resulting material was fragile enough to be manually milled. Details of the activation process and room temperature hydriding are provided in the next section below.

2. Experimental

Ingots of U–Mo alloy with 10 wt%Mo were induction melted into a magnesia-stabilized zirconia crucible. Metallic uranium and metallic molybdenum were used as raw materials. Metallic uranium was produced by magnesiothermic reduction [15,16] and 99.95% purity metallic molybdenum was provided by Alfa Aesar as cylinders measuring 3 mm in diameter and 3 mm in height. Both materials were charged inside the zirconia crucible and heated by induction under a high-purity argon atmosphere up to melting. The melting temperature was maintained for 3 min providing homogenization, after which the furnace was turned off, allowing the alloy to solidify inside the crucible.

The solid material was a cylindrical piece measuring close to 40 mm in diameter by 50 mm in height, weighing around 1200 g with a density of 16.87 g/cm^3. The ingot was treated at 1000 °C for 72 h inside a reactor under pure argon and quickly cooled for retention of the gamma phase. For cooling, the reactor was removed from the furnace and forced air was applied with the aid of a fan. It was then cut in pieces to study the powder preparation process by hydriding–milling–dehydriding (HMD).

Small pieces (4–5 g) were taken from the U–Mo ingot. These pieces were cleaned in a solution of nitric acid diluted in water, followed by washing in water and then in anhydrous ethanol. As-cleaned samples were immediately mounted inside the hydrogen reactor and evacuated at 0.1 Pa. A Sieverts-type apparatus (built at the laboratory) was used to detect hydrogen absorption by the sample. In this apparatus, pressure was monitored by digital pressure gauges, together with sample temperature and time. Data were stored in a PLC connected to a computer. After connecting the reactor to the apparatus, the whole gas line, including the reactor, was purged with argon and hydrogen in sequence. Sample temperature was monitored by a thermocouple inside the reactor, located just above the sample holder, which was enveloped by a copper case especially designed to provide better temperature homogeneity in the whole sample.

Activation consisted of heating the sample under pressurized hydrogen (0.8 MPa) at 15 °C/min up to 700 °C for 1 h. The reactor was then evacuated at this temperature for 5 min and pressurized again to 0.8 MPa. This was done to remove volatile impurities from the sample surface. At this point the gas supply was cut off. Cooling was achieved by removing the reactor from the furnace and assisted with forced air cooling (fan). After reaching room temperature under hydrogen pressure, the sample was evacuated again (0.01 Pa), heated up to 300 °C at 5 °C/min and maintained at this temperature for 1 h, which was enough to complete the hydrogen desorption.

Following this activation procedure, the sample was allowed to cool at room temperature, always under a high vacuum (0.01 Pa). Hydrogen was then introduced in the reactor at a constant rate (9 mL/min) assured by a mass flow controller. Pressurization occurred up to 0.6 MPa, followed by a depressurization stage at the same rate. Powdering the hydrided sample was performed in a separate experiment following room-temperature hydriding. To achieve this, the reactor was opened inside a glove-box with a protective argon atmosphere and controlled oxygen and humidity. Hydrided samples were easily comminuted to a −150 mesh size by manual operation using a stainless steel mortar. After collecting some powder for characterization, the reactor was charged with this powdered material, closed and finally connected again to the Sieverts apparatus for dehydriding following the procedure described above. The dehydrided samples were then removed from the reactor inside the glove-box.

X-ray diffraction was conducted on heat-treated ingot samples (before hydriding), as well as hydrided and dehydrided particles using Cu Kα radiation. HMD powder particles were also characterized by SEM analysis.

3. Results and discussion

Fig. 1 shows the hydrogen pressure variation during sample cooling from 700 °C (HMD route). After removing the reactor from

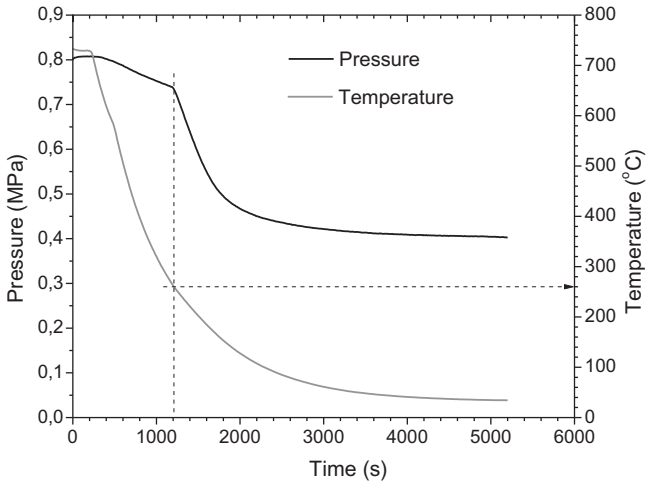

Fig. 1. Pressure variation (relative or gauge) in the reactor during cooling from 700 °C under static hydrogen atmosphere (activation).

the furnace, the pressure begins to decrease, as does the temperature. A small part of this decrease is due to system leakage. A significant change in the pressure rate drop can be clearly observed when the temperature reached 260 °C, indicating hydrogen uptake by the sample.

At room temperature, the dehydrided sample started to absorb hydrogen at 0.160 MPa (Fig. 2). At this point, a pressure drop (down to 0.053 MPa) was observed, since the hydrogen flow rate provided by the flow controller was lower than the uptake rate of the sample (the maximum flow rate of the controller was 10 mL/min). At the depressurizing stage, pressure varied linearly with time, denoting no dehydriding of the sample. This means that the process is not reversible at room temperature.

An accurate measurement of the hydrogen absorbed by the sample at room temperature was achieved by performing a blank experiment (with no sample) conducted under the same conditions, i.e. hydrogen flow rate and temperature. We then subtracted this data from the hydriding sample curve (pressurization stage). The resultant curve (sample – blank) is presented in Fig. 3a. Both terminal portions of this curve are linear with a slight inclination. These inclinations are due to a small volume difference between sample pressurization and blank pressurization, since in the blank

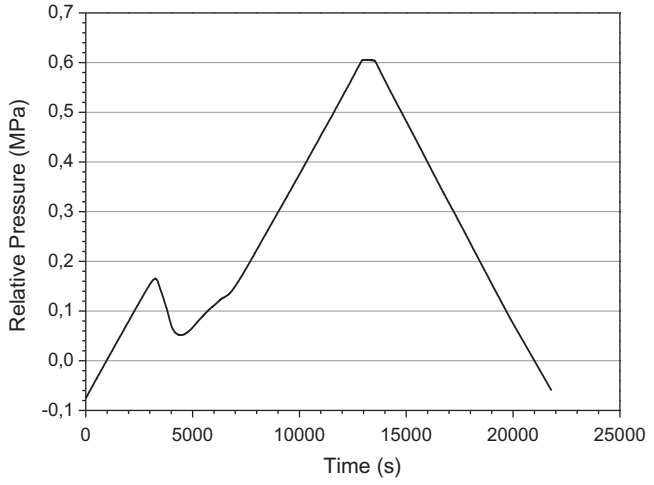

Fig. 2. Pressure variation (relative or gauge) in the reactor at room temperature (25 °C) under constant hydrogen flow (9 mL/min).

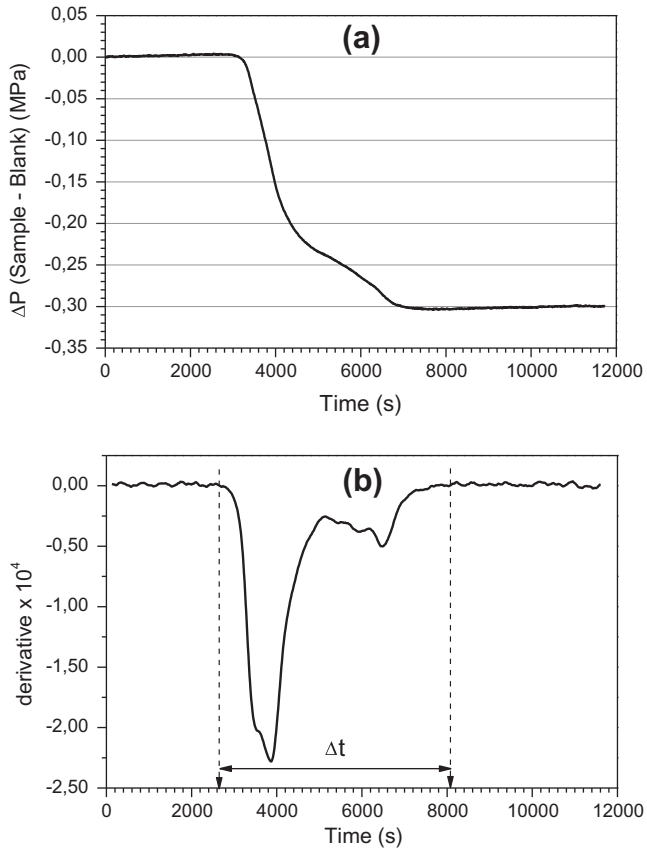

Fig. 3. (a) Pressure difference (ΔP) curve at room temperature and (b) derivative curve showing the time interval (Δt) for hydrogen absorption measurement.

experiment, no sample was charged in the reactor (sample volume is 0.26 cm^3 regarding a sample with 4,5 g). The total volume available for hydrogen filling (~221 cm^3) was slightly higher than in the sample experiment (221–0.26 cm^3), demanding more time to attain the same pressure. The quantity of hydrogen absorbed by the sample was measured by determining the time interval (Δt) between the two linear terminal portions in the pressure difference curve (actually an absorption curve), which is more accurately verified in the correspondent derivative curve showed in Fig. 3b. The following expression was used then:

$$(\Delta P_{(\text{Sample}-\text{Blank})}/\Delta PBlank) \times \text{IGF} \quad (1)$$

where $\Delta P_{(\text{Sample - Blank})}$ is the pressure difference observed in sample–blank curve (Fig. 3a), ΔP_{Blank} is the pressure difference observed in the blank curve (not shown here) and IGF is the integrated gas flow obtained directly from the gas flow controller, all of them between the time interval previously determined. $\Delta P_{(\text{Sample - Blank})}/\Delta P_{\text{Blank}}$ is a kind of correction factor, since during the hydrogen absorption rate of the sample is different from the pressurization rate of the blank curve (this factor would be "1" if the both rates were the same, which would result in a plateau in the sample curve during hydriding).

Following this procedure and expressing the quantity of hydrogen as a molar fraction, we determined a value of 71.2%, corresponding to a H/M ratio of = 2.47, considering the nominal chemical composition of the sample (U-10 wt%Mo). These result is lower comparing to the work from Pasqualini et al. [10] who identified a U-7Mo hydride with a H/M ratio >2.8, but not at room temperature. According to Chen et al. [11] an increasing hydrogen absorption was verified during the first eight hydriding cycles at room temperature. We should have in mind that H/M ratio

obtained here was after the second hydriding cycle (the first one was at the activation procedure), so this value could be higher if we would have performed more cycles.

X-ray diffraction patterns from as heat-treated (before hydriding), hydrided and dehydrided samples are presented in Fig. 4. Heat-treated sample exhibits some texture (the first peak of gamma phase should be higher than the others). Texture was expected since we carried out XRD analysis on no powdered samples and use a diffraction equipment without spinning sample holder. After hydriding, an amorphous-like pattern was observed (pattern b in Fig. 4), as well as the reflections of the UO phase. Gamma U-10 wt%Mo phase reflections were not detected after hydriding, which indicates a complete transformation following hydrogen absorption. After dehydriding, the gamma phase structure was observed again.

Concerning the amorphous-like pattern, we initially believed that no hydride was formed, as previously reported [14]. This is supported by the fact that uranium hydrides (the two main allotropes alpha UH_3 [17] and beta UH_3 [18]) are crystalline. Moreover, Pasqualini et al. [10] reported that their hydride was crystalline and with beta UH_3 structure. Thus, instead of hydride formation, we considered the possibility that the hydrogen atoms were diffused in the U-10 wt%Mo solid solution. In this case, the hydrogen intake would have strained the gamma BCC crystal lattice, causing a large broadening of the X-ray reflections.

However, thermodynamic calculations of the maximum hydrogen content that could be dissolved in a U-10 wt%Mo solid solution do not support that previous analysis. To do so we used the thermodynamic approach described by Powell [19]. According to that, for the reaction

$$1/2H_2 \leftrightarrows H_M \tag{2}$$

occurring at an hydrogen gas pressure of P_{H2}, where H_M is the concentration of hydrogen dissolved in the alloy, the equilibrium constant K_H may be written as

$$\ln K_H = \ln\left\{\frac{\gamma_H[H_M]}{P_{H_2}^{1/2}}\right\} = \ln\left[N\frac{(1+Ae^{-B/T})}{(2\sinh[C/(2T)])^3}\right] - \ln\left[\frac{J_{H_2}T^{7/4}}{(1-e^{L_{H_2}/T})^{1/2}}\right] + \frac{E-M_{H_2}}{T} \tag{3}$$

where γ_H is the activity coefficient (~1 at infinity dilution), N is the degeneracy of dissolved hydrogen sites per unit concentration at 0 K and at infinite dilution (=3 for octahedral site occupation), $A = 20$, $B = 4200$ K, $C = 1684$ K, $J_{H2} = 0.02073$, $L_{H2} = 5978$ K, $E = 28477$ K and $M_{H2} = 25997.5$ K. At $T = 300$ K and $P_{H2} = 0.160$ MPa, Eq. (3) gave us a value of H_M of only 1.37% (molar fraction). So the solid solution explanation had to be discarded. A new possible hypothesis was then formulated to explain the amorphization of a hydride that is usually crystalline. According to this new proposed hypothesis, the amorphization could be related to the fact that hydriding gamma U–Mo solid solution does not result in fine particulate material, like that observed with pure uranium hydriding. Actually gamma phase is only cracked after hydriding and not pulverized like alpha uranium phase.

Alpha uranium has a orthorhombic lattice (oC4 or A20) and a density of 19.04 g/cm^3 [20,21], while the stable and more common form of UH_3 (beta type) is cubic (cP8 or A15) with a density of 10.91 g/cm^3 [21,22]. These structures are represented in Fig. 5a and d, respectively. It is known that the crystal lattice of the metallic alpha uranium suffers severe internal strain and structural changes when it is hydrided [23] and this fact is used to produce fine uranium metal particles after dehydriding [22]. Thus in the α-U to β-UH_3 transformation, anisotropic stresses may originate due to the orthorhombic to cubic transformation, with a volume increase of 68.3%. When the low temperature form of the UH_3 (alpha) is considered (Fig. 5c), with a density of 11.12 g/cm^3 [22], the volume increase is 71.5%. Whatever the volume increase, the stress level arising from this swelling would cause generalized fracture, which results in extremely fine powder particles.

Something different should occur in the hydriding gamma U–Mo alloy (BCC, Fig. 5b). The U–Mo solid solution has tensile internal stresses caused by substitutional molybdenum atoms that are smaller than uranium atoms. Hydriding imposes compression stresses as hydrogen atoms occupy interstitial sites, together with

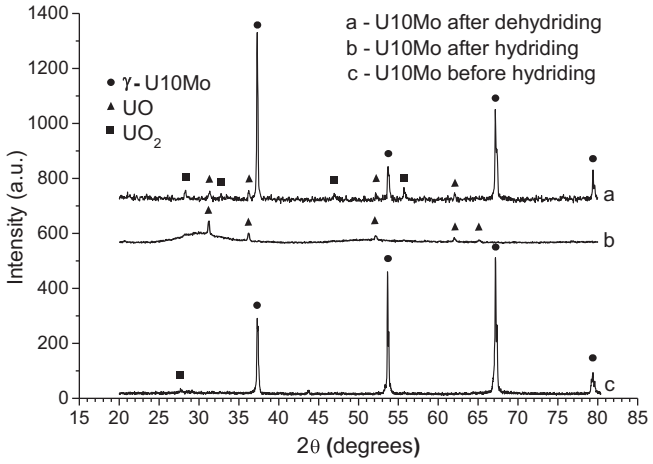

Fig. 4. X-ray diffraction patterns of as heat-treated (before hydriding), hydrided and dehydrided samples.

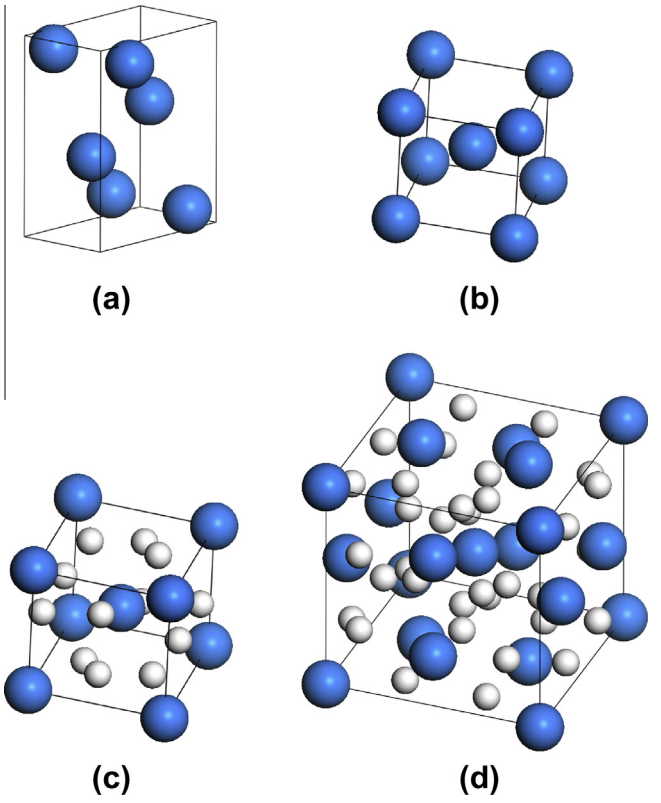

Fig. 5. Unit cells drawings of: (a) alpha uranium; (b) gamma uranium; (c) alpha UH_3 and (d) beta UH_3. Uranium and hydrogen atoms are represented by larger and smaller balls, respectively.

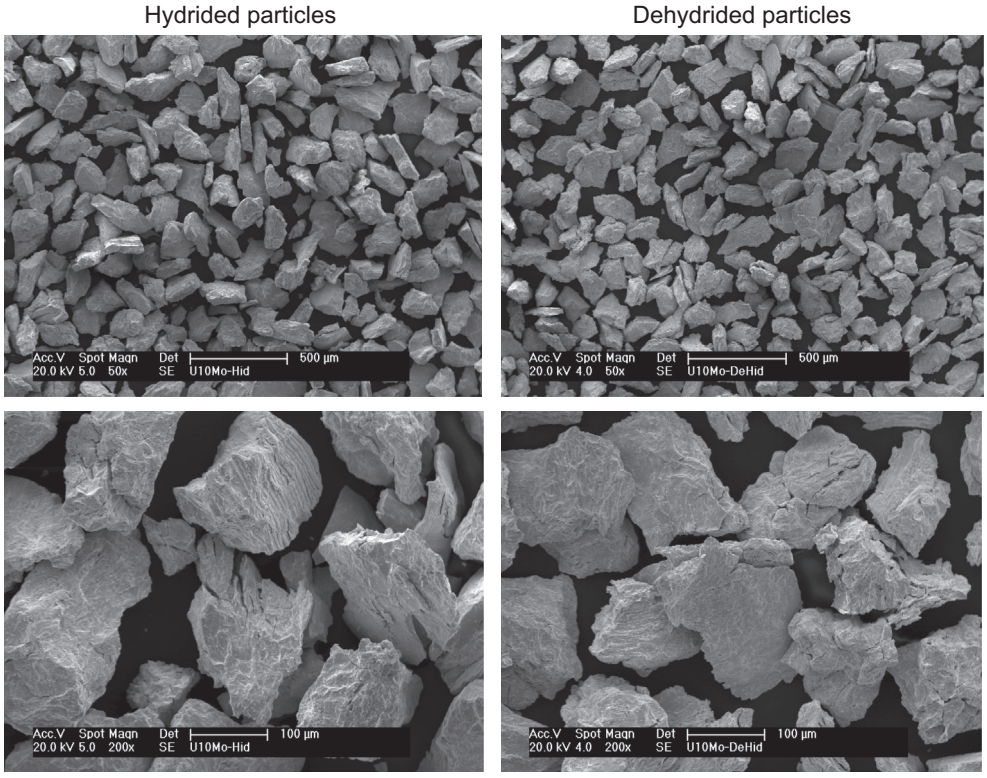

Fig. 6. SEM micrographs (secondary electrons images) of hydrided and dehydrided U-10 wt%Mo powder particles.

shear stresses, since interstitial sites in the BCC lattice are irregular. Part of this compression stress field is counterbalanced by the tensile stress field of the solution, which means that the U–Mo lattice is more able to resist hydriding (volume expansion) than the orthorhombic lattice of alpha uranium. In addition, the transformation of the gamma solid solution to alpha or beta $(U,Mo)H_3$ implies an isotropic volume increase, since all the lattices involved are cubic (Fig. 5).

We assume that hydriding a gamma U–Mo alloy will produce equivalent hydride allotropes to those observed when hydriding metallic uranium. Since here the hydriding operation was performed at room temperature, a mixture of alpha and beta $(U,Mo)H_3$ is expected, with prevalence for the latter (70% in the case of UH_3, as estimated by Mulford et al. [17]). In order to calculate the volume increase verified in the transformation of gamma solid solution to beta $(U,Mo)H_3$, we took in account our experimental data based on the lattice constants of the solid solution (measured by DRX analysis) and the density of the hydride measured by helium picnometry, since the amorphous pattern impaired conventional DRX measurements. Our gamma U–Mo phase has a cubic unit cell with $a_0 = 0.34112$ nm, which is in good agreement with the values determined by Seong et al. [24]. The calculated density is then 17.28 g/cm^3. The measured density of the amorphous hydride was 10.19 g/cm^3, resulting in a volume increase of 69.6%. This is a little bit higher than the expansion calculated for the alpha uranium to beta UH_3. However, in the case of U–Mo solid solution, the stresses are supported by the lattice, since the expansion is isometric and some part is counterbalanced by the lattice itself. Thus, the U–Mo lattice is severely strained by hydrogen intake, broadening the X-ray reflections.

Fig. 6 shows some SEM micrographs took from hydrided and dehydrided powder particles (−100 + 150 mesh size range). Particle shape was very similar in both cases. Most particles are regular and equiaxial, but some of them exhibit a platelet shape. This could be the result of a preferential crack plane, countering the amorphization hypothesis. Conchoidal fracture markings, typical of an amorphous material, were also not observed on the surface of the particles. Thus, a nanocrystalline hydride formation should be considered. It should be noticed that both small crystallite size and microstrains can cause broadening of the X-ray peaks, as seen on Fig. 4 (pattern b). Further, some cracks on the surface of the particles can be seen, denoting fragile behavior following hydriding.

4. Conclusions

We were able to produce U-Mo powder with appropriate granulometry by simple manual grinding. Hydriding gamma U-10 wt%Mo alloy was achieved at room temperature following a thermal activation treatment. The resulting hydrided material appears to be amorphous or nanocrystalline. Although no gamma phase was observed following hydrogen absorption, the dehydrided material presented the BCC structure from gamma phase again. A hypothesis for the amorphization (or nanocrystallization) of the hydrided alloy was formulated based on the high strains developed during hydriding, but without the severe or bulk rupture of the hydrided material observed when hydriding pure uranium. The majority of the powder particles produced by the HMD route is equiaxial, though it contains some flat particles.

Acknowledgments

The authors are grateful to FAPESP and CNPq for the research grants (2007/50018-2, 2007/07769-7, 2011/13849-9, 471008/2011-7, 470363/2012-6 and 481079/2008-4) provided for this work. The authors would also like to thank Dr. E. E. Pasqualini for his cooperative and encouraging discussions and MSc. R.B. Falcão and E.D.C.C. Dammann for their assistance with the Sieverts apparatus and data collection.

References

[1] J.L. Snelgrove, G.L. Hofman, M.K. Meyer, C.L. Trybus, T.C. Wiencek, Nucl. Eng. Des. 178 (1) (1997) 119–126.

[2] G.L. Hofman, J.L. Snelgrove, S.L. Hayes, M.K. Meyer, Progress in development of low-enriched U–Mo dispersion fuels, in: 6th International Topical Meeting on Research Reactor Fuel Management (RRFM 2002), European Nuclear Society, Ghent, Belgium, April 21–25. p. 50–58. (<http://www.euronuclear.org/meetings/rrfm/pdf/RRFM%202002.pdf>).

[3] K.H. Kim, D.B. Lee, C.K. Kim, G.E. Hofman, K.W. Paik, J. Nucl. Mater. 245 (2–3) (1997) 179–184.

[4] C.R. Clark, B.R. Muntifering, J.F. Jue, Production and characterization of atomized U–Mo powder by the rotating electrode process, in: Proceedings of the 2007 International Meeting on Reduced Enrichment fot Research and Test Reactors, Prague, Czech Republic, September 23–27, 2007. (<http://www.rertr.anl.gov/RERTR29/PDF/15-2_Clark.pdf>).

[5] C.R. Clark, M.K. Meyer, Fuel powder production from ductile uranium alloys, in: Proceedings of the 1998 International Meeting on Reduced Enrichment for Research and Test Reactors, São Paulo, Brazil, October 18–23,1998. (<http://www.rertr.anl.gov/Fuels98/CClark.pdf>).

[6] H.Vacelet, P. Sacristan, A. Languille,Y. Lavastre, M. Grasse, Irradiation of full size UMo plates, in: Proceedings of the 1999 International Meeting on Reduced Enrichment for Research and Test Reactors, Budapest, Hungary, October 3–8, 1999. (<http://www.rertr.anl.gov/Web1999/PDF/07vacelet99.pdf>).

[7] S. Balart, P. Bruzzoni, M. Granovsky, L. Gribaudo, J. Hermida, J. Ovejero, G. Rubiolo, E. Vicente, U–Mo alloy powder obtained by a hydride–dehydride process, in: Proceedings of the 2000 International Meeting on Reduced Enrichment for Research and Test Reactors, Las Vegas, Nevada, October 1–6, 2000. (<http://www.rertr.anl.gov/Web2000/PDF/Balar00.pdf>).

[8] M. Solonin, A.V. Vatulin, Y.A. Stetsky, Y.I. Trifonov, B.D. Rogozkin, Development of the method of high density fuel comminution by hydride–dehydride processing, in: Proceedings of the 2000 International Meeting on Reduced Enrichment for Research and Test Reactors, Las Vegas, Nevada, October 1–6, 2000. (<http://www.rertr.anl.gov/Web2000/PDF/Vatu00.pdf>).

[9] L. Olivares, J. Marin, J. Lisboa, H. Pesenti. Powder production of uranium–molybdenum–metal alloys applying hydride–dehydride methodology, in: Proceedings of the 2008 International Meeting on Reduced Enrichment for Research and Test Reactors, Washington, D.C.,October 5–9, 2008. (<http://www.rertr.anl.gov/RERTR30/pdf/S10-5_Olivares.pdf>).

[10] E.E. Pasqualini, J.H. Garcia, M. Lopez, E. Cabanillas, P. Adelfang, Powder Production of U–Mo Alloy by HMD Process.(Hydriding–Milling–Dehydriding), in: 6th International Topical Meeting on Research Reactor Fuel Management (RRFM 2002), European Nuclear Society, Ghent, Belgium, April 21-25, p. 183–187. (<http://www.euronuclear.org/meetings/rrfm/pdf/RRFM%202002.pdf>).

[11] M. Chen, X. Yi-fu, W. Jing, J. Jia, P. Zhang, J. Nucl. Mater. 400 (1) (2010) 69–72.

[12] X. Yi-Fu, M. Chen, W. Jing, C. Chen, Fusion Eng. Des. 85 (7–9) (2010) 1492–1495.

[13] S. Dubois, J. Noirot, J.M. Gatt, M. Ripert, P. Lemoine, P. Boulcourt, Comprehensive overview on iris program: irradiation tests and pie on high density UMo/Al dispersion fuel, in: 11th International Topical Meeting on Research Reactor Fuel Management (RRFM 2007), European Nuclear Society, Lyon, France, March 12–14, 2007. (<http://www.euronuclear.org/meetings/rrfm2007/transactions/rrfm2007-transactions-session-3.pdf>).

[14] M. Durazzo, C.J. Rocha, J. Mestnik Filho, R.M. Leal Neto, Powdering ductile U–Mo alloys for nuclear dispersion fuel, in: 14th International Topical Meeting on Research Reactor Fuel Management (RRFM 2010), European Nuclear Society, Marrakech, Morocco, March 21–25, 2010. (<http://www.euronuclear.org/meetings/rrfm2010/transactions/RRFM2010-poster.pdf>).

[15] M. Durazzo, A. Silva, J. de Souza, E. de Carvalho, H. Riella, Current status of U_3Si_2 fuel elements fabrication in Brazil, in: Proceedings of the 2007 International Meeting on Reduced Enrichment fot Research and Test Reactors, Prague, Czech Republic, September 23–27, 2007. (<http://www.rertr.anl.gov/RERTR29/PDF/11-8_Durazzo.pdf>).

[16] A.M. Saliba Silva, I.C. Martins, L.R. dos Santos, D.G. da Silva, E.F. Urano de Carvalho, H.G. Riella, M. Durazzo, Metallic Uranium Production for Irradiation Targets Alloys: in 15th International Topical Meeting on Research Reactor Fuel Management (RRFM 2011), European Nuclear Society, Rome, Italy, March 20–24, 2011. p. 232–240. (<http://www.euronuclear.org/meetings/rrfm2011/transactions/transactions-poster.pdf>).

[17] R.N.R. Mulford, F.H. Ellinger, W.H. Zachariasen, J. Am. Chem. Soc. 76 (1) (1954) 297–298.

[18] R.E. Rundle, J. Am. Chem. Soc. 73 (9) (1951) 4172–4174.

[19] G.L. Powell, J. Phys. Chem. 83 (5) (1979) 605–613.

[20] B.M. Ma, Nuclear Reactor Materials and Applications, Van Nostrand Reinhold Company, 1983.

[21] T.B. Massalski, H. Okamoto, Binary Alloy Phase Diagrams, ASM International, 1990.

[22] W.M. Mueller, P. James Blackledge, G.G Libowitz, Metal Hydrides, Academic Press, 1968.

[23] T. Hashino, Y. Okajima, J. Phys. Chem. 77 (18) (1973) 2236–2241.

[24] B.S. Seong, C.H. Lee, J.S. Lee, H.S. Shim, J.H. Lee, K.H. Kim, C.K. Kim, V. Em, J. Nucl. Mater. 277 (2-3) (2000) 274–279.